SUPPORTING INFORMATION

Marker-free phenotyping of tumor cells by fractal analysis of RICM images

*Katharina Klein, Timo Maier, Vera C. Hirschfeld-Warneken and Joachim P. Spatz**

Department of New Materials and Biosystems, Max Planck Institute for Intelligent Systems, and Department of Biophysical Chemistry, University of Heidelberg;

postal address: Heisenbergstr. 3, 70569 Stuttgart, Germany

MATERIAL & METHODS

Cell Culture

Two pancreatic cell lines derived from the same metastasis of a pancreatic adenocarcinoma named Patu8988t (PatuT) and Patu8988s (PatuS) were obtained from the German collection of microorganisms and cell cultures (DSMZ). The cells were grown in DME (Dulbecco modified Eagle) medium 31885 supplemented with 5 % FBS (fetal bovine serum; Life technologies) and 5 % HS (horse serum; Sigma) at 37°C and 5 % CO_2. The culture medium was exchanged every 2 to 3 days. Cells were grown to 70-80 % confluence and were then treated with 2.5 %

trypsin/EDTA (Gibco) and centrifuged (1200 rpm, 3 min). For RICM experiments $75x10^3$ cells were cultured in 2 ml medium with 1 % serum. Staining was performed with Cell Tracker Red or Cell Tracker Blue ® (Life technologies) within the culture flasks for 45 min before treating cells with trypsin solution, followed by centrifugation.

Substrate Coating

Glass coverslips (20x20 mm; Carl Roth) were cleaned in Piranha solution (hydrogen peroxide (H_2O_2) and concentrated sulfuric acid (H_2SO_4) at a ratio of 1:3) for 60 min, then rinsed with MilliQ® water and blown dry with nitrogen. Coverslips were then incubated with collagen (collagen type I, rat tail, Harbor Bio-products) at a concentration of 100 µg/ml in 0.02 N acetic acid for 30 min at room temperature. The coverslips were rinsed with MilliQ® water and PBS buffer after the coating step.

Reflection Interference Contrast Microscopy (RICM)

2λ-RICM Setup

The RICM setup was implemented on an inverted microscope Olympus IX71 (Olympus) equipped with an antiflex 63x oil immersion objective (NA 1.25, NeofluarAntiflex; Zeiss). Samples were illuminated by a fiber-coupled Xenon lamp (R 100W/45C OFR; Osram) that is coupled to the microscope via a cage system composed of a lens, an iris to minimize the stray light, and a dichroic mirror. The RICM reflector cube within the microscope consists of a polarizer, a dichroic mirror, and an analyzer. The orange light was filtered by a bandpass filter (593/40; AHF Analysetechnik) before it was imaged by a 12 bit CCD camera (Orca-R2; Hamamatsu). The entire cage system was covered with a custom-built light protection system to

ensure good image quality with high contrast. The microscope itself was enclosed by a heated and air humidified custom-built chamber.

Theory

Image contrast of RICM results from the interference of light that is reflected at several refractive index boundaries. The reflected rays interfere and give rise to an interference pattern, which allows an estimation of the object's contour (Fig. 1B). The intensity distribution of the interference pattern for objects in the (x,y) plane at a given wavelength λ can be described by:

$$I(h(x,y),\lambda) = I_1 + I_2 + 2\sqrt{I_1 I_2}\cos\left(\frac{4\pi n h(x,y)}{\lambda} + \delta\right) \qquad \text{Equation 1}$$

where $I(h(x,y),\lambda)$ is the intensity on the interferogram at point (x,y) with its height $h(x,y)$. I_1 and I_2 are the intensities of the two interfering beams, n is the refractive index of the medium and δ is the phase shift of the light reflected from the object, which is equal π if $n_{object} > n_{buffer}$. In the case that the two interfaces are close together the interferogram shows a minimum. When the membrane is further away from the substrate the path difference increases and the corresponding intensity on the interferogram also increases. From the cosine in the interference function it is obvious that the interference pattern repeats periodically every $\Delta h = \lambda/2n$. By adding a second or accessorily a third wavelength the ambiguity of about $\lambda/2$ in the interference pattern can be elided through comparison of the interferograms, allowing calculation of absolute distances.[1 2]

RICM Experiments

Cells were seeded on collagen-coated glass surfaces within the microscopy chamber. RICM images of single cells were performed 60 min after seeding.

Data Analysis of RICM Images

Data analysis was performed with the MATLAB software (R2007b, 1994-2011 The MathWorks, Inc.). Based on an algorithm from the cell segmentation toolbox, the analysis was modified for RICM images.

Fractal Analysis of RICM Images

For fractal analysis the ImageJ plug-in „FracLac_2.5q“ (A. Karperien, FracLac for ImageJ, Version 2.5, 1999-2007) was used. For estimating the FD the dimension D_b describing the ratio of increasing detail with increasing scale (ε) was determined using the box-counting method. The basic procedure is to systematically lay a series of square grids of variable length (ε) over an image and count the number of squares (N(ε)) necessary to cover the image. This process is repeated for different ε and the D_b can be calculated using the formula: $D_b = -\lim_{\varepsilon \to 0} [\log (N(\varepsilon))/\log(\varepsilon)]$. The FD can be estimated as the slope of the regression line for a log-log plot of N (ε) over ε. For preprocessing, the RICM images (image size of 1344x1024 pixels) were cropped according to the cell area on the RICM images to one of four set image sizes (320x320, 500x500, 600x600, or 650x650 pixels). Two independent parameters and the combination of both were tested to get the fractal dimension of the sister cell lines on the basis of the RICM images: 1. contour of the cell (on the basis of binary images); 2. topology of the cell without inclusion of the cell´s contour (on the basis of RICM images = grayscale images); 3. contour and topology of the cell (on the basis of RICM images = grayscale images). For the first approach we applied the standard box-counting scan, whereas for the approaches with gray-scale images we used the differential box-counting method.[3] The differential box-counting method is like the standard method, except that the image binarization step is avoided and gray-scale can be analyzed. For

all scans we used 12 grid positions and a maximum box size of 45 % of ROI. We also left the maximum number of boxes to 0 for the default. The minimum box size for the first approach was set to 10 pixels, for the other two approaches with the grayscale images it was set to 2 pixels.

Modeling and Mathematical Test

All mathematical analysis, including fitting and statistical analysis, was performed with the software OriginPro8.6G (OriginLab, Northampton, MA). In all cases the mean value with its respective standard error is shown. Statistics: Values of the FD for the two cell lines were compared using an ANOVA one- way analysis, after testing for normal distribution with a Kolmogorov-Smirnov test. Differences between mean values of every cell line were considered statistically significant at a p value of less than 0.001.

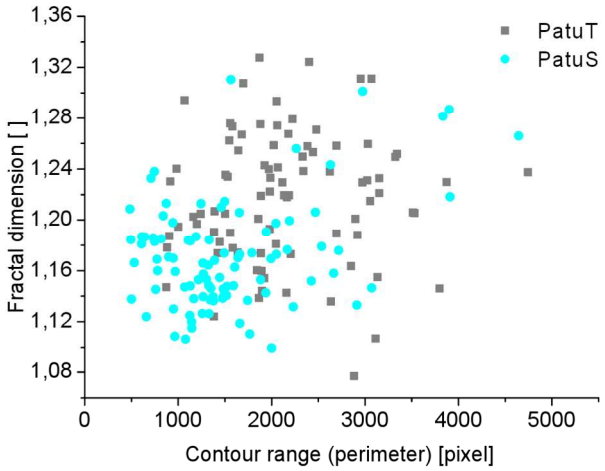

Figure S1. Independence of fractal dimension and cell size. In the scatter plot the fractal dimension is plotted as a function of the diameter of the contour.

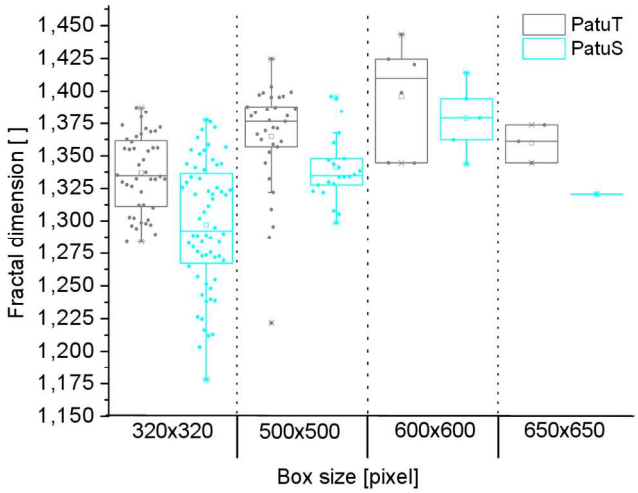

Figure S2. Independence of fractal dimension and image size. Image preprocessing for fractal analysis included cropping the RICM images to one of four different image sizes depending on the cell size. For all box sizes the FD of PatuT cells is higher. In the boxplot the box shows 50 % of the data, the whisker an interquartile range of 1.5x, and the small rectangle represents the mean value.

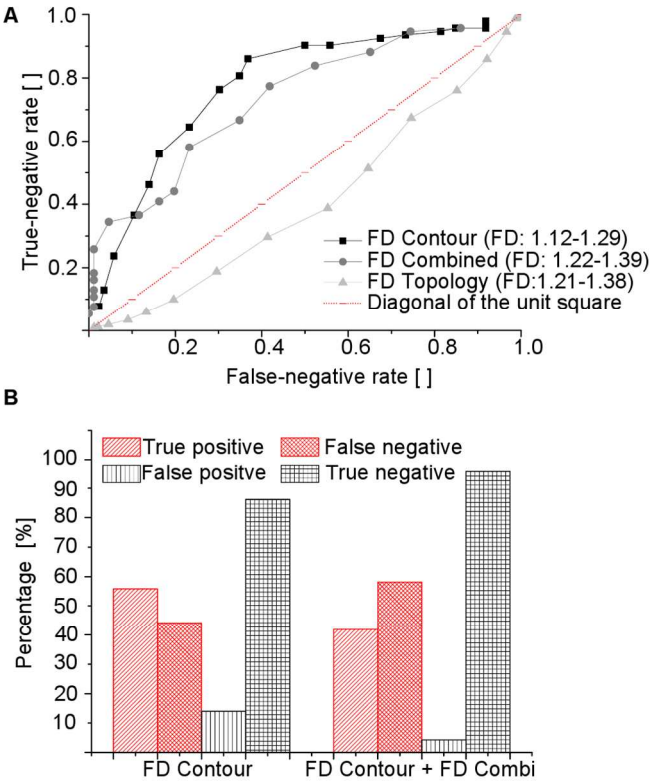

Figure S3. ROC analysis.(A) ROC curves indicate the classification performance of different FDs obtained by analyzing the cell contour, the topology, or the combined aspects prioritizing the readouts for PatuS cells. (B) With a successive second analysis,which included all PatuS cells identifiedby the FD contour parameter (Threshold FD =1.21), using a second parameter termed FD combined (Threshold FD = 1.33) the percentage of the false positive rate could be reduced from 14 to 4 %. (N_{PatuT}=86, N_{PatuS}=93 cells)

Screening of additional cell lines

Additional experiments were performed on further malignant cell lines of pancreas, breast and bladder carcinoma. As shown in figure S4.a contour analysis of PANC-1 pancreas cells, reveals a distribution of the fractal dimension values between 1.08 and 1.32, similar to those of PatuT cells. In general the contour of MCF7 breast tumor cells is showing a comparable distribution of FD values, whereas the values of HT-1197, a malignant but poorly differentiated bladder tumor line, are shifted towards lower FD with a much narrower distribution between 1.10 and 1.24.

Fractal dimension of the adhesion topology (figure S4.b) of PANC-1 cells could be determined to be in between 1.20 - 1.36, in consistence with the values obtained for PatuT. While the fractal dimension of MCF7 lies within the same interval, HT-1197 cells show a much broader distribution between 1.16 and 1.40 with a definitive double peak at around 1.23 and 1.32. This is related to the distinctive ring structures in the RICM images of HT-1197 cells (figure S5), where boxes close to the outer edge can be identified with lower FD and boxes near the center of the cell with higher. Such distinct ring structures were characteristic for more than 95% of all HT-1197 cells but could neither be observed for MCF7 nor for PANC-1.

For the combined analysis of contour and adhesion topology (figure S4.c) a FD distribution of PANC-1 was obtained to be between 1.30 and 1.44 with a peak of about 1.37, precisely on the level of PatuT. In contrast, both MCF7 and HT-1197 show distributions shifted towards lower or higher FD. In case of MCF7, the fractal dimension lies in between 1.24 and 1.42 while HT-1197 shows an FD of about 1.36 - 1.48 with a peak at around 1.43, thereby allowing a clear discrimination between the different cell types.

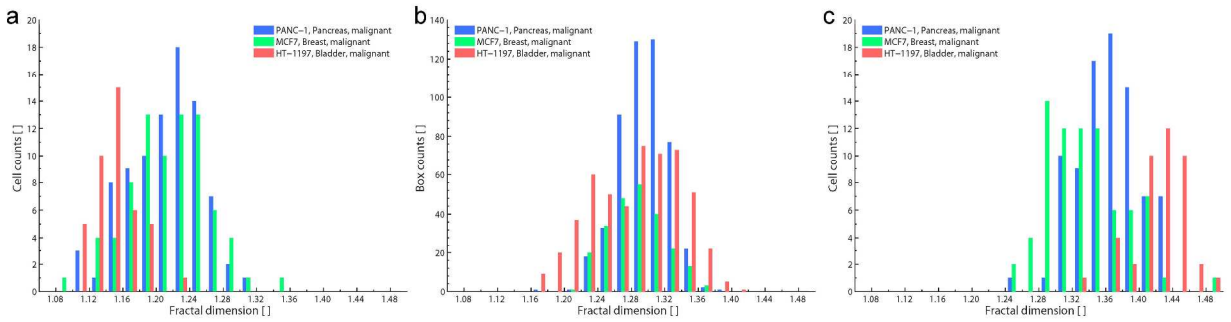

Figure S4: Fractal dimension of PANC-1, MCF7 and HT-1197 malignant tumor cells in case of contour (a), adhesion topology (b) or combined contour and adhesion topology analysis (c) (N_{PANC-1}=86, N_{MCF7}=78 cells $N_{HT-1197}$=42).

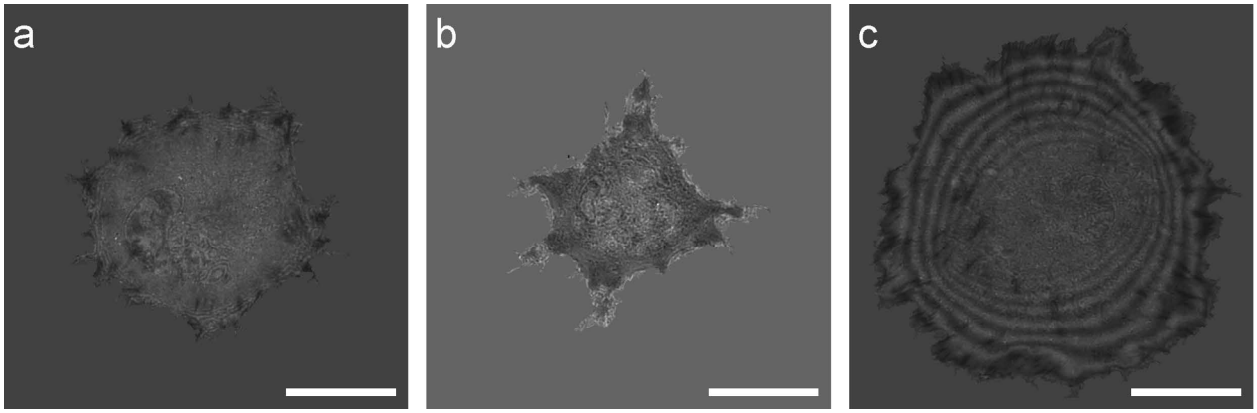

Figure S5: Selected RICM images of PANC-1 (a), MCF7 (b) and HT-1197 (c) malignant tumor cells. Distinct Ring structures could only be seen for HT-1197 cells and were clearly related to the FD of the adhesion topology. Scale bar: 20 µm.

REFERENCES

1. Picart, C.; Sengupta, K.; Schilling, J.; Maurstad, G.; Ladam, G.; Bausch, A. R.; Sackmann, E. *J Phys Chem B* **2004,** *108* (22), 7196-7205.

2. Schilling, J.; Sengupta, K.; Goennenwein, S.; Bausch, A. R.; Sackmann, E. *Phys Rev E* **2004,** *69* (2).

3. Karperien, A. *FracLac for ImageJ - FracLac Advanced User´s Manual*, Charles Sturt University, Australia: **2004-5**.